

# Enveloped Eyewall Lightning: The EEL Signature in Tropical Cyclones

CHRIS VAGASKY

*Vaisala Inc., Louisville, Colorado*

(Manuscript received July 17, 2017; review completed October 10, 2017)

## ABSTRACT

A variety of strategies are employed to monitor the strength and track of tropical cyclones, including aircraft reconnaissance and satellite. Recent developments to lightning location systems have provided another tool for monitoring tropical systems over the ocean at long distances from land. Vaisala's Global Lightning Dataset (GLD360) has uniform global coverage with high detection efficiency, providing highly detailed observations of tropical cyclone lightning events. GLD360 has allowed the discovery of a unique lightning signature within the eyewall of some significant tropical cyclones, named the Enveloped Eyewall Lightning (EEL) signature. This signature refers to lightning that completely envelops the eyewall and persists for at least six hours. The mechanisms behind this signature are not yet known. To facilitate future research into the EEL signature, GLD360 lightning stroke data surrounding 82 global tropical cyclones that reached an intensity of  $58.1 \text{ m s}^{-1}$  (113 kt) or greater between 2012 and 2015 were analyzed to create a catalog of EEL signatures. A total of 32 tropical cyclones were found with the signature and can be used in future studies to understand this newly identified feature of enveloped eyewall lightning.

## 1. Introduction

There are a number of strategies to monitor the strength and track of tropical cyclones (TCs), including aircraft reconnaissance, satellite, and radar. Aircraft reconnaissance is typically limited to the Atlantic Basin. Satellite data are available globally, and allow forecasters to monitor TC development, strength, and track far from land, but can have coarse temporal and spatial resolutions. As a TC approaches land, forecasters can use radar for higher resolution monitoring of intensity and track, including Doppler estimates of wind speed, and tracking convective elements within the eyewall and outer bands. These convective elements can have greater impacts if they make landfall, including higher wind speeds, greater rainfall, and occasionally tornadoes. In recent years, long-range lightning location systems (LLS) have enabled forecasters to monitor convective elements in TCs around the world in near real-time.

Lightning in TCs was once thought to be relatively uncommon because ice and supercooled water are rarely simultaneously present within the eyewall region of hurricanes (Black and Hallett 1986). LLS have found lightning in TCs to be a more common event than previously thought. This resulted in an interest to understand how the location, frequency, and time trend of lightning in a TC may provide information about its intensity.

One of the first published studies of TC lightning comes from Lyons and Keen (1994), who found lightning primarily in the outer rain bands, and a minimum in the inner core of mature TCs. It is important to note that many of the early studies on TC lightning were conducted on systems within 400–500 kilometers of the United States coast (Molinari et al. 2006). Prior to 2004, LLS were primarily used for detecting lightning over landmasses. Long-range LLS, including the Worldwide Lightning Location Network (WWLLN; Lay et al. 2004), the Long-Range Lightning Detection

Network (Demetriades and Holle 2005), and the Global Lightning Dataset (GLD360; Said et al. 2010) enabled the detection of lightning over the oceans away from landmasses.

With lightning data available over the oceans, applications for this data to assist forecasters in nowcasting TCs became evident. Demetriades and Holle (2006) examined six Atlantic TCs between 2003 and 2005, and suggested the importance of continuous monitoring of convective structures in TCs. They suggest that using lightning data can help forecasters monitor for rapid intensification, identify regions with the highest wind speeds and heaviest rainfall, and issue appropriate advisories and warnings. Leary and Ritchie (2009) and Mazzarella and Ritchie (2014) used lightning data over the Eastern Pacific Ocean to identify cloud clusters that were more likely to develop into TCs. They found that cloud clusters that developed into TCs had up to 2.84 times more frequent lightning than the non-developing clusters. As lightning data over the oceans became more available, lightning within the eyewall of TCs was seen more frequently, and studies of eyewall lightning outbreaks followed.

Convective bursts in the eyewall can indicate a change in the TC's path (Willoughby 1990); eyewall lightning outbreaks can indicate the beginning or ending of an intensification period (Molinari et al. 1999); rapid intensification, an eyewall replacement cycle, or the maximum intensity period (Squires and Businger 2008); or impending landfall (Zhang et al. 2012). Molinari et al. (1999) also suggest that the lack of lightning in the inner core of a TC may indicate a steady-state system. DeMaria et al. (2012) examined WLLN data in all North Atlantic and East Pacific TCs between 2005 and 2010. Their results suggest high lightning density in the inner core precedes rapid weakening of Atlantic TCs and are similar to results published by Jiang and Ramirez (2013). Using the Tropical Rainfall Measuring Mission Lightning Imaging Sensor (TRMM LIS), Jiang and Ramirez suggest a negative correlation between inner core lightning and TC intensification. These sometimes conflicting findings suggest that there is still much to be learned about how lightning in the inner core of a TC can be used to help nowcast or forecast these systems.

Early notification of TC intensification can help forecasters issue better warnings for areas susceptible to damage (Price et al. 2009). Their paper reviewed 58 TCs around the world between 2005 and 2007 that reached maximum winds of  $58.1 \text{ m s}^{-1}$  (113 kt) or greater, and lightning in a  $10^\circ \times 10^\circ$  box surrounding the

system. Fifty-six of those TCs showed “statistically significant positive correlations between lightning activity and sustained winds,” with lightning peaking before the maximum wind in more than 70% of the cases. This suggests that lightning may be an indicator of TC intensification and could be used for nowcasting and forecasting purposes.

The findings of Price et al. (2009) are similarly seen in studies from Abarca et al. (2011), Bovalo et al. (2014), and Zhang et al. (2015). Abarca et al. (2011) used WLLN data to look at 24 TCs in the Atlantic Basin, and found that intensifying TCs had up to twice as many lightning flashes in the inner core as TCs that did not intensify. Using WLLN data in the Southwest Indian Ocean, Bovalo et al. (2014) studied 70 TCs between 2005 and 2013. Periods of increased lightning activity were found to be correlated with periods of rapid intensity change in those TCs. Zhang et al. (2015) analyzed 116 TCs in the Northwest Pacific Ocean between 2005 and 2009. Using WLLN lightning data, they found the greatest lightning density in the inner core was found in storms that would intensify by  $14.9\text{--}24.7 \text{ m s}^{-1}$  (29–48 kt) in the following 24 hours. These four studies would seem to suggest a potential to predict rapid intensity changes in TCs based on an increase in lightning.

In recent years, GLD360 has detected lightning fully enveloping the eyewall of several significant TCs for extended periods of time, including 2013 Supertyphoon Haiyan and 2014 Supertyphoon Hagupit (Pessi 2015). The author of this manuscript further noticed Hurricane Patricia (2015) and Supertyphoon Nepartak (2016) as exhibiting the same phenomenon. The goal of this paper is to introduce the Enveloped Eyewall Lightning (EEL) signature and its potential utility as a tool for monitoring TCs by operational meteorologists. The study to follow catalogs global TCs between 2012 and 2015 with a maximum one-min sustained wind speed of  $58.1 \text{ m s}^{-1}$  (113 kt) or greater, and lightning that envelops the eyewall for a period of six hours or longer, which is named the Enveloped Eyewall Lightning signature.

## 2. Data and methods

Global TCs between 2012 and 2015 with one-min sustained winds of  $58.1 \text{ m s}^{-1}$  (113 kt) or greater at any point during their lifetime were selected for analysis. The threshold of  $58.1 \text{ m s}^{-1}$  (113 kt) was selected to narrow the TC search results. The author initially hypothesized the EEL signature would only be evident in the strongest TCs, supported by his experience

identifying the signature in Hurricane Patricia (2015), Supertyphoon Nepartak (2016), and the results of Pessi (2015). The best track center locations for the selected TCs were overlaid on the surrounding lightning data using QGIS ([www.qgis.com](http://www.qgis.com)).

#### a. Lightning data

Lightning data for this study come from Vaisala's GLD360 (Fig. 1), a ground-based LLS capable of detecting lightning over land and oceans globally. The operating principle of GLD360 is detailed in Said et al. (2010). GLD360 uses a network of long-range lightning detection sensors tuned to the Very Low Frequency (3–30 kHz) band. Using Time-of-Arrival and Magnetic Direction Finding techniques, and an empirical waveform bank, GLD360 detects and geolocates individual lightning events (Said et al. 2010). The location algorithm that generates the GLD360 dataset was updated in 2015, with data prior to the update reprocessed using the new algorithm (Said and Murphy 2016). Using Vaisala's National Lightning Detection Network (NLDN) as ground truth, Said and Murphy (2016) found the reprocessed GLD360 dataset to have a relative cloud-to-ground (CG) flash detection efficiency (DE) of 75–85%, and a median location accuracy of 1.8 km over the United States. Rudlosky et al. (2017) compared the reprocessed GLD360 dataset to TRMM LIS. Their results found that GLD360 detected more than 60% of LIS flashes between 2012 and 2015 over the National Hurricane Center Atlantic marine forecast areas, and suggest GLD360 can be used to investigate Atlantic basin TCs.

#### b. Best track information

TC best track information was selected from the International Best Track Archive for Climate Stewardship (IBTrACS; Knapp et al. 2010). The IBTrACS database collects best-track data from twelve Regional Specialized Meteorological Centers and Tropical Cyclone Warning Centers, including The Australian Bureau of Meteorology, NOAA's National Hurricane Center (NHC), and the United States Department of Defense Joint Typhoon Warning Center (JTWC). Different forecast agencies use different wind speed averaging periods when discussing a storm's intensity (Knapp et al. 2010) and can make interagency comparisons difficult. Harper et al. (2010) provides guidance for converting between wind averaging periods, but this can introduce errors. Therefore, IBTrACS

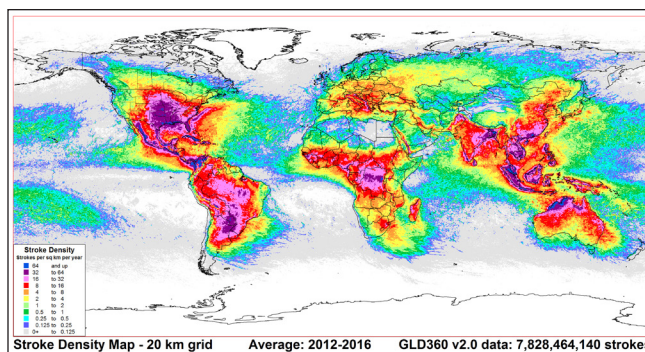


**Figure 1.** Global map showing the annual average lightning stroke density on a 20 km grid using reprocessed GLD360 data from 1 January 2012 – 31 December 2016, and illustrates the ability of GLD360 to detect lightning across all regions of the globe. Areas of higher stroke density are colored in red, pink, and purple, whereas regions of lower stroke density are colored in gray and blue. *Click image for an external version; this applies to all tables and figures hereafter.*

presents the original data from each agency, allowing users to develop their own methods for selecting which intensity data to use. Knapp et al. (2010) also present a table of recent TC climatology research and show that HURDAT (HURricane DATabase; Jarvinen et al. 1984) and JTWC (Chu et al. 2002) best-track data are most frequently used in global TC climatology reviews. This paper uses HURDAT from NHC for North Atlantic and East Pacific storms, and JTWC for the West Pacific, South Pacific, South Indian, and North Indian basins; both list wind speeds as one-min averages. Both HURDAT and JTWC data are included in the IBTrACS database.

#### c. Methodology

The University of North Carolina – Asheville hosts a user-friendly version of IBTrACS ([www.atms.unca.edu/ibtracs/ibtracs\\_current/browse-ibtracs/browseibtracs.php](http://www.atms.unca.edu/ibtracs/ibtracs_current/browse-ibtracs/browseibtracs.php)). For each year in the study period, TC best-track data were reviewed for each of the six TC basins. Chosen candidate storms were any TC with a peak HURDAT or JTWC wind speed of  $58.1 \text{ m s}^{-1}$  (113 kt) or greater during its lifetime. A total of 82 candidate storms were selected from the IBTrACS database from a total of 389 TCs globally between 2012 and 2015. Table 1 shows statistics of total TCs and selected TCs for each year in the study period.

For ease in collecting lightning data for each candidate storm, the following method was used to

**Table 1.** Statistics of the number of global Tropical Cyclones (TCs) and selected TCs for each year and overall during the period of study.

	2012	2013	2014	2015	Total
<b>Total TCs</b>	91	103	92	103	389
<b>Category 4 and 5 TCs</b>	14	14	22	32	82
<b>Percentage</b>	15.4	13.6	23.9	31.1	21.1

create a lightning domain and gather the lightning data:

- List the best-track latitude and longitude values from smallest to largest
- Subtract 3 degrees from the minimum values and add 3 degrees to the maximum values, creating  $Lat_{min}$ ,  $Lon_{min}$ ,  $Lat_{max}$ , and  $Lon_{max}$  values
- The lightning domain is bounded by the coordinates  $(Lat_{min}, Lon_{min})$ ,  $(Lat_{min}, Lon_{max})$ ,  $(Lat_{max}, Lon_{min})$ , and  $(Lat_{max}, Lon_{max})$
- The GLD360 database was queried within the lightning domain from the beginning time to ending time of each candidate storm

Substantially more lightning data than required were generated through this technique, but it gave full visibility to lightning within the inner core and outer rain bands of each candidate TC.

Lightning data were received as an ASCII file for each candidate storm, with each lightning event identified by the UTC date and time (milliseconds) of occurrence, its latitude and longitude (ten-thousandths of degrees), and its magnitude (kiloamperes) and polarity. Said et al. (2013) discusses the method of estimating lightning magnitude and polarity in GLD360. Using QGIS, the lightning data were plotted and color-coded by day, and the best-track data were plotted and color-coded by wind speed. As an example of this technique, Fig. 2 shows the lightning domain, lightning data, and best-track data of Hurricane Patricia (2015). Each candidate storm's plotted data were visually inspected for evidence of an EEL signature.

A candidate storm was determined to have an EEL signature if the plotted archived lightning data formed a continuous path that completely surrounded at least two best-track data points (Fig. 3). The requirement that the continuous lightning path includes two best-track data points limits the EEL events to long-lasting lightning outbreaks that previous studies (e.g., Abarca et al. 2011,

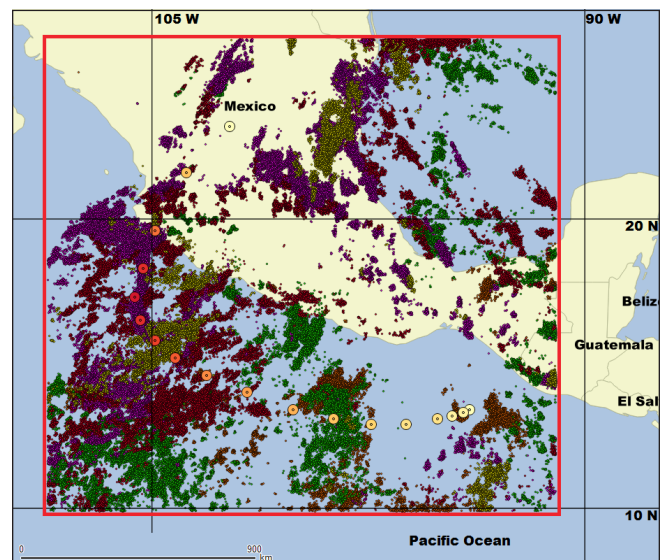


**Figure 2.** Map showing the lightning domain (red polygon outlining extent of GLD360 lightning stroke data), Hurricane Patricia best track data (filled circles color-coded by wind speed), and individual GLD360 lightning strokes (small dots color-coded by day).

DeMaria et al. 2012) have found to be uncommon. This also allows for future analysis to be completed using information available from best-track data. Lightning that envelops the eyewall of TCs and persists for less than six h was observed (e.g., Hurricane Matthew 2016), but attempting to identify or catalog all instances of this more transient eyewall lightning outbreak is beyond the scope of this paper.

### 3. Analysis and discussion

A total of 32 TCs (Table 2) were identified that exhibited the EEL signature, with 18 occurring in the West Pacific. EEL signature TCs occurred in all basins (Fig. 4) and in all years (Table 3), with EEL duration ranging from approximately 9 h to 75 h (median 27 h; Table 2). Figure 5 shows EEL signatures from the West Pacific, North Atlantic, North Indian, and South Indian

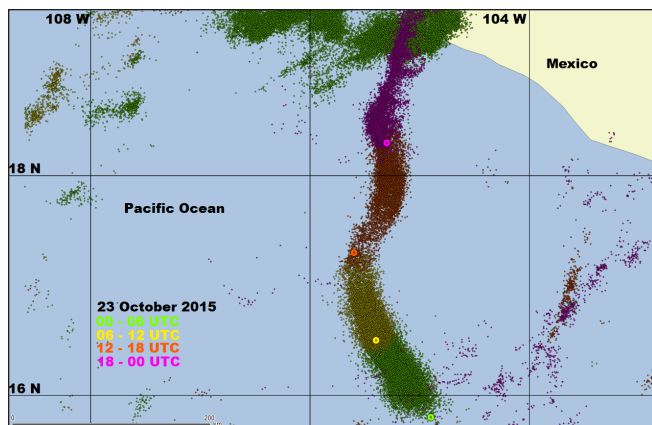


**Figure 3.** Zoomed in map of Hurricane Patricia GLD360 lightning stroke data (small colored dots) and best-track data (filled circles), illustrating the EEL signature. Lightning stroke data and best-track data are color-coordinated. This figure shows lightning and best-track locations between 0000-2359 UTC 23 October 2015.

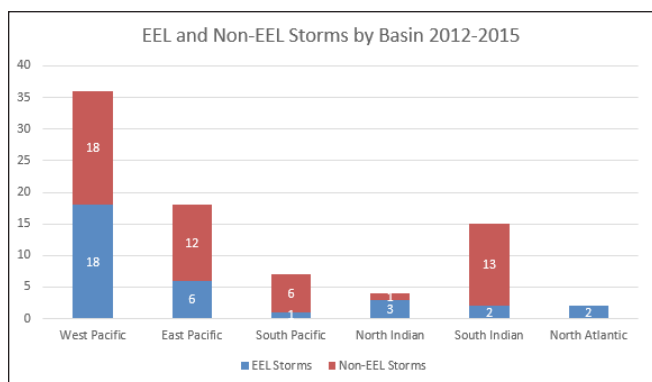


**Figure 4.** The quantities of EEL and non-EEL storms per basin from the candidate tropical cyclones during the study period. There were only two candidate storms in the North Atlantic between 2012 and 2015, and both exhibited the EEL signature.

basins, and demonstrates the potential utility of using GLD360 lightning data to monitor TCs over the open oceans.

As discussed in the introduction, studies of inner core and eyewall lightning outbreaks have not yielded consistent results. Some studies have suggested these lightning outbreaks are coincident with storm intensification (e.g., Molinari et al. 1999, Squires and Businger 2008), although some suggest storm weakening (e.g., DeMaria et al. 2012, Jiang and Ramirez 2013). Thirty of the thirty-two storms identified with EEL signatures intensified during the period of time with enveloped eyewall lightning. Identification of the EEL

signature may provide forecasters a visual indicator that a TC is beginning an intensification period. Figure 6 compares the intensity of EEL signature TCs when the EEL signature appears, when the signature dissipates, and the storm's peak intensity during the EEL signature.

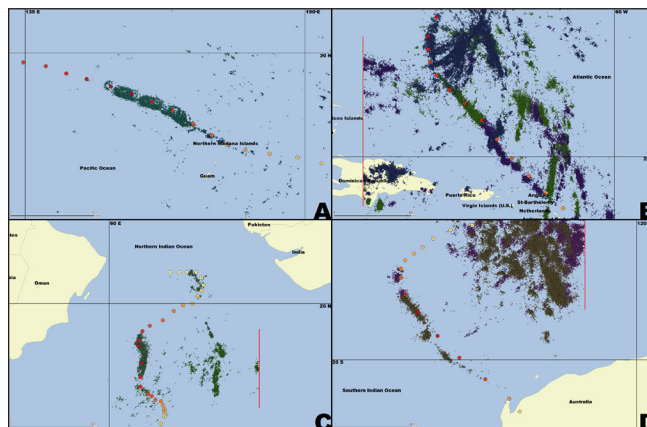


**Figure 5.** Maps illustrating examples of EEL signatures from the West Pacific [A; Soudelor (2015)]; North Atlantic [B; Gonzalo (2014)]; North Indian [C; Nilofar (2014)]; South Indian [D; Quang (2015)] basins. As with Fig. 3, the filled circles represent best-track data, and the small dots are GLD360 lightning strokes on the days of the EEL signature's presence. The vertical red lines in 5b-d represent the end of the lightning data domain.

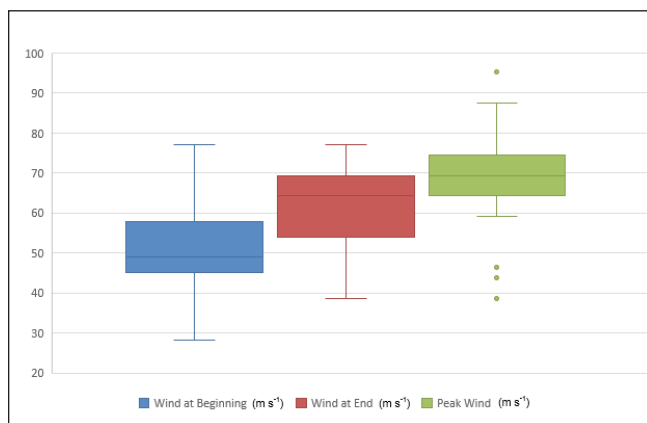


**Figure 6.** Box and whisker plots showing the wind speed ( $\text{m s}^{-1}$ ) of EEL storms at the beginning (blue) and end (red) of the EEL signature. The peak intensity of the storm when the EEL signature was present is the green plot. In 30 of the 32 EEL storms, the intensity of the storm increased, with one storm [Maysak (2015)] weakening, and one storm [Dolphin (2015)] remaining the same intensity.

**Table 2.** A list of the 32 tropical cyclones that exhibited the EEL signature. The storms are listed alphabetically by year of development, with maximum wind speed in meters per second, approximate duration of the EEL signature, and basin of formation listed.

TC Name	Year	Peak Wind Speed [m s <sup>-1</sup> (kt)]	Duration (h)	Basin
<a href="#">Guchol</a>	2012	66.9 (130)	60	West Pacific
<a href="#">Jelawat</a>	2012	66.9 (130)	30	West Pacific
<a href="#">Sanba</a>	2012	79.7 (155)	42	West Pacific
Danas	2013	61.7 (120)	18	West Pacific
Francisco	2013	72.0 (140)	66	West Pacific
<a href="#">Haiyan</a>	2013	87.5 (170)	72	West Pacific
<a href="#">Lekima</a>	2013	72.0 (140)	27	West Pacific
<a href="#">Phailin</a>	2013	69.5 (135)	21	Northern Indian
<a href="#">Usagi</a>	2013	69.5 (135)	45	West Pacific
<a href="#">Utor</a>	2013	66.9 (130)	54	West Pacific
Genevieve	2014	72.0 (140)	42	East Pacific
Gonzalo	2014	64.3 (125)	75	North Atlantic
<a href="#">Hagupit</a>	2014	79.7 (155)	72	West Pacific
Marie	2014	72.0 (140)	12	East Pacific
<a href="#">Nilofar</a>	2014	59.2 (115)	36	Northern Indian
<a href="#">Nuri</a>	2014	72.0 (140)	18	West Pacific
<a href="#">Vongfong</a>	2014	79.7 (155)	24	West Pacific
Bansi	2015	72.0 (140)	36	Southern Indian
Chapala	2015	66.9 (130)	18	Northern Indian
Dolphin	2015	72.0 (140)	12	West Pacific
Hilda	2015	64.3 (125)	45	East Pacific
In Fa	2015	61.7 (120)	21	West Pacific
Joaquin	2015	69.5 (135)	24	North Atlantic
<a href="#">Maysak</a>	2015	77.2 (150)	21	West Pacific
<a href="#">Nangka</a>	2015	69.5 (135)	18	West Pacific
<a href="#">Noul</a>	2015	72.0 (140)	36	West Pacific
Olaf	2015	59.2 (115)	9	East Pacific
Pam	2015	77.2 (150)	21	South Pacific
Patricia	2015	95.2 (185)	30	East Pacific
<a href="#">Quang</a>	2015	61.7 (120)	12	Southern Indian
Sandra	2015	66.9 (130)	36	East Pacific
<a href="#">Soudelor</a>	2015	79.7 (155)	27	West Pacific

TCs with the EEL signature tend to be intensifying when it appears and reach a peak intensity during the EEL signature. The intensity of the TC then tends to decrease towards the end of the EEL signature lifecycle. In three storms, the peak wind speed during the EEL signature was less than 51.4 m s<sup>-1</sup> (100 kt), and warrants future review. However, the median peak wind speed during an EEL signature was 69.5 m s<sup>-1</sup> (135 kt).

Figure 7 compares the overall peak intensity of TCs with the EEL signature to TCs without the EEL signature. There is an artificial lower bound of 59.2 m s<sup>-1</sup> (115 kt) for both EEL and non-EEL TCs based on the minimum intensity requirement for this study and

how wind speeds are reported in best-track data. The frequency of EEL signatures in storms weaker than 58.1 m s<sup>-1</sup> (113 kt) is unknown, and is worthy of future study. Finally, the peak intensity of EEL signature storms [median = 70.7 m s<sup>-1</sup> (137.5 kt), n = 32] was significantly greater (Mann-Whitney U = 394.5, p < 0.001 two-tailed) than that of non-EEL signature storms [median = 64.3 m s<sup>-1</sup> (125 kt), n = 50].

Although this study used archived GLD360 lightning data and best track TC data from IBTrACS to identify and catalog EEL signatures, the signature was originally identified using real-time lightning data. Figure 8 shows 4 panels of how the EEL signature

**Table 3.** Statistics of the number of candidate TCs that exhibited the Enveloped Eyewall Lightning (EEL) signature for each year and overall during the period of study.

	2012	2013	2014	2015	Total
<b>Category 4 and 5 TCs</b>	14	14	22	32	82
<b>EEL Storms</b>	3	7	7	15	32
<b>Percentage</b>	21.4	50	31.8	46.9	39.0

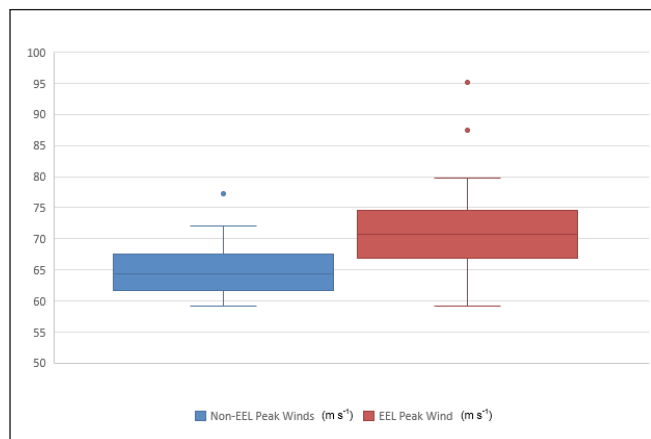


**Figure 7.** Box and whisker plots comparing the peak intensity of non-EEL storms (blue) to the peak intensity of EEL-storms (red). The 25th-percentile of EEL storms is nearly the same intensity of the 75th-percentile of non-EEL storms [ $66.9 \text{ m s}^{-1}$  (130 kt) versus  $67.5 \text{ m s}^{-1}$  (131 kt)].

appears in real-time lightning data during Hurricane Patricia (2015). Identification of the EEL signature by tropical forecasters can provide confirmation of the storm's location and potential intensity in near real-time.

GLD360 is believed to be the only LLS that can identify the EEL signature, particularly at locations far from land. This expectation comes from the greater flash DE offered by GLD360 and its uniform global coverage. Networks with DE that decrease with increasing distance from land will detect and locate less lightning over the open oceans, resulting in a limited view of the lightning in TCs, including in the eyewall. The Geostationary Lightning Mapper on the GOES-16 satellite is reported to have similar DE to GLD360 (Goodman et al. 2013), but it has just begun collecting data, so it remains to be seen what signatures will emerge in TC lightning with this new instrument.

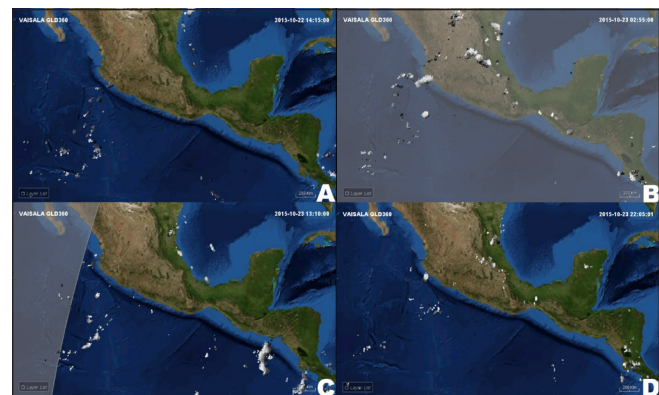


**Figure 8.** Four-panel plot showing the evolution of Hurricane Patricia's EEL signature in a real-time lightning view. Evolution goes left to right, top to bottom. Time is in UTC. The sloped line in panel C is the day-night terminus. In panel A, Patricia's EEL signature has yet to develop, but is apparent in the last panels B, C, and D, through landfall in panel D. Loop courtesy of Dr. Ryan Said. *Click image for a 1:07 loop of GLD360 lightning data.*

#### 4. Conclusion

Using lightning data from GLD360, 82 global tropical cyclones (TCs) between 2012 and 2015 with peak wind speeds of  $58.1 \text{ m s}^{-1}$  (113 kt) or higher were analyzed for periods of enveloped eyewall lightning (EEL). Lightning data and the EEL signature have potential utility as a near real-time tool for monitoring the location, track, and intensity of TCs at ranges beyond aircraft reconnaissance and Doppler radar. A total of 32 TCs from across all basins were found to have the EEL signature, which is defined as a signature of detected lightning in which lightning completely envelops the eyewall of a TC and persists for at least six h. The TCs that exhibited the EEL signature tended to be stronger than those TCs without the EEL signature. The median peak wind speed of EEL signature storms was  $70.7 \text{ m s}^{-1}$  (137.5 kt), whereas it was  $64.3 \text{ m s}^{-1}$  (125 kt) for non-EEL signature storms.

Although the mechanisms behind the EEL signature are not known yet, this study provides a selection of TCs with the EEL signature that can be used for future research. These unique events can be used to help meteorologists develop a better understanding of lightning within a TC.

*Acknowledgments.* This study was initially performed as part of the degree requirements of the Mississippi State University Applied Meteorology Program. I wish to thank my colleagues at Vaisala for supporting this endeavor, including Drs. Martin Murphy, Kevin Petty, and Ryan Said; Dario Atallah, Bill Brooks, Ron Holle, and Lee Nelson. Many thanks also to my reviewers for improving the clarity and readability of this manuscript.

## REFERENCES

- Abarca, S. F., K. L. Corbosiero, and D. Vollaro, 2011: The World Wide Lightning Location Network and convective activity in tropical cyclones. *Mon. Wea. Rev.*, **139**, 175–191, [CrossRef](#).
- Black, R. A., and J. Hallett, 1986: Observations of the distribution of ice in hurricanes. *J. Atmos. Sci.*, **43**, 802–822, [CrossRef](#).
- Bovalo, C., C. Barthe, N. Yu, and N. Bègue, 2014: Lightning activity within tropical cyclones in the South West Indian Ocean. *J. Geophys. Res. Atmos.*, **119**, 8231–8244, [CrossRef](#).
- Chu, J.-H., C. R. Sampson, A. S. Levine, and E. Fukada, 2002: The Joint Typhoon Warning Center tropical cyclone best-tracks, 1945–2000. Naval Research Laboratory Rep. NRL/MR/7540-02-16, 22 pp. [Available online at [www.usno.navy.mil/NOOC/nmfc-ph/RSS/jtwc/best\\_tracks/TC\\_bt\\_report.html](http://www.usno.navy.mil/NOOC/nmfc-ph/RSS/jtwc/best_tracks/TC_bt_report.html).]
- DeMaria, M., R. T. DeMaria, J. A. Knaff, and D. Molenaar, 2012: Tropical Cyclone Lightning and Rapid Intensity Change. *Mon. Wea. Rev.*, **140**, 1828–1842, [CrossRef](#).
- Demetriades, N. W. S., and R. L. Holle, 2005: Long-range lightning applications for hurricane intensity. *Preprints, Conf. on Meteor. Appl. Of Lightning Data*, San Diego, Jan. 9–13, Amer. Meteor. Soc., 9 pp. [Available online at [ams.confex.com/ams/pdfpapers/84498.pdf](http://ams.confex.com/ams/pdfpapers/84498.pdf).]
- , and —, 2006: Long range lightning applications for tropical cyclones. *Preprints, Second Conf. on Meteor. Appl. Of Lightning Data*, Atlanta, Jan. 29–Feb. 2, Amer. Meteor. Soc., 9 pp. [Available online at [ams.confex.com/ams/pdfpapers/99183.pdf](http://ams.confex.com/ams/pdfpapers/99183.pdf).]
- Goodman, S. J., and Coauthors, 2013: The GOES-R Geostationary Lightning Mapper (GLM). *J. Atmos. Res.*, **125–126**, 34–49, [CrossRef](#).
- Harper, B. A., J. D. Kepert, and J. D. Ginger, 2010: Guidelines for converting between various wind averaging periods in tropical cyclone conditions. WMO/TD-No. 1555. [Available online at [www.wmo.int/pages/prog/www/tcp/documents/WMO\\_TD\\_1555\\_en.pdf](http://www.wmo.int/pages/prog/www/tcp/documents/WMO_TD_1555_en.pdf).]
- Jarvinen, B. R., C. J. Neumann, and M. A. S. Davis, 1984: A tropical cyclone data tape for the North Atlantic basin, 1886–1983: Contents, limitations and uses. NOAA Tech. Memo. NWS NHC-22, 24pp. [Available online at [www.nhc.noaa.gov/pdf/NWS-NHC-1988-22.pdf](http://www.nhc.noaa.gov/pdf/NWS-NHC-1988-22.pdf).]
- Jiang, H., and E. Ramirez, 2013: Necessary Conditions for Tropical Cyclone Rapid Intensification as Derived from 11 Years of TRMM Data. *J. Climate*, **26**, 6459–6470, [CrossRef](#).
- Knapp, K. R., M. C. Kruk, D. H. Levinson, H. J. Diamond, and C. J. Neumann, 2010: The International Best Track Archive for Climate Stewardship (IBTrACS): Unifying tropical cyclone data. *Bull. Amer. Meteor. Soc.*, **91**, 363–376, [CrossRef](#).
- Lay, E. H., R. H. Holzworth, C. J. Rodger, J. N. Thomas, O. Pinto Jr., and R. L. Dowden, 2004: WWLL global lightning detection system: Regional validation study in Brazil. *Geophys. Res. Lett.*, **31**, L03102, [CrossRef](#).
- Leary, L. A., and E. A. Ritchie, 2009: Lightning flash rates as an indicator of tropical cyclone genesis in the eastern North Pacific. *Mon. Wea. Rev.*, **137**, 3456–3470, [CrossRef](#).
- Lyons, W. A., and C. S. Keen, 1994: Observations of lightning in convective supercells within tropical storms and hurricanes. *Mon. Wea. Rev.*, **122**, 1897–1916, [CrossRef](#).
- Mazzarella, L. A. L., and E. A. Ritchie, 2014: Determining Hurricane Formation in the eastern North Pacific using the Global Lightning Dataset 360 and the Long-Range Lightning Detection Network. *23rd Intl. Lightning Detection Conf.*, Tucson, Arizona, Mar. 18–21, Vaisala, 6pp. [Available online at <https://my.vaisala.net/Vaisala%20Documents/Scientific%20papers/2014%20ILDC%20ILMC/ILMC-Thursday/Mazzarella%20and%20Ritchie-Determining%20Hurricane%20Formation%20Using%20the%20GLD%20360%20and%20the%20Long-Range%20LDN-2014-ILDC-ILMC.pdf>.]
- Molinari, J., P. Moore, and V. Idone, 1999: Convective structure of hurricanes as revealed by lightning locations. *Mon. Wea. Rev.*, **127**, 520–534, [CrossRef](#).
- , N. W. S. Demetriades, R. L. Holle, and D. Vollaro, 2006: Applications of long-range lightning data to hurricane formation and intensification. *Preprints, Second Conf. on Meteor. Appl. Of Lightning Data*, Atlanta, Jan. 29–Feb. 2, Amer. Meteor. Soc., 2pp. [Available online at [ams.confex.com/ams/pdfpapers/103732.pdf](http://ams.confex.com/ams/pdfpapers/103732.pdf).]

- Pessi, A., 2015: Evolution and Characteristics of Lightning Distribution over Typhoon Haiyan (2013). *7th Conf. Meteor. Appl. Lightning Data*, Phoenix, Amer. Meteor. Soc., 10.4. [Available online at [ams.confex.com/ams/95Annual/webprogram/Paper255145.html](http://ams.confex.com/ams/95Annual/webprogram/Paper255145.html).]
- Price, C., M. Asfur, and Y. Yair, 2009: Maximum hurricane intensity preceded by increase in lightning frequency. *Nat. Geosci.*, **2**, 329–332, [CrossRef](#).
- Rudlosky, S. D., M. J. Peterson, and D. T. Kahn, 2017: GLD360 Performance Relative to TRMM LIS. *J. Atmos. Oceanic Technol.*, **34**, 1307–1322, [CrossRef](#).
- Said, R. K., and M. J. Murphy, 2016: GLD360 Upgrade: Performance analysis and applications. *24th Intl. Lightning Detection Conf.*, San Diego, Apr. 8–21, Vaisala, 8pp. [Available online at <https://my.vaisala.net/Vaisala%20Documents/Scientific%20papers/2016%20ILDC%20ILMC/Ryan%20Said%20and%20Martin%20Murphy.%20GLD360%20Upgrade%20Performance%20Analysis%20and%20Applications.pdf>]
- \_\_\_\_\_, U. S. Inan, and K. L. Cummins, 2010: Long-range lightning geolocation using a VLF radio atmospheric waveform bank. *J. Geophys. Res.*, **115**, D23108, [CrossRef](#).
- \_\_\_\_\_, M. B. Cohen, and U. S. Inan, 2013: Highly intense lightning over the oceans: Estimated peak currents from global GLD360 observations. *J. Geophys. Res. Atmos.*, **118**, 6905–6915, [CrossRef](#).
- Squires, K., and S. Businger, 2008: The morphology of eyewall lightning outbreaks in two category 5 hurricanes. *Mon. Wea. Rev.*, **136**, 1706–1726, [CrossRef](#).
- Willoughby, H. E., 1990: Temporal changes of the primary circulation in tropical cyclones. *J. Atmos. Sci.*, **47**, 242–264, [CrossRef](#).
- Zhang, W., Y. Zhang, D. Zheng, and X. Zhou, 2012: Lightning distribution and eyewall outbreaks in tropical cyclones during landfall. *Mon. Wea. Rev.*, **140**, 3573–3586, [CrossRef](#).
- \_\_\_\_\_, \_\_\_\_\_, \_\_\_\_\_, F. Wang, and L. Xu, 2015: Relationship between lightning activity and tropical cyclone intensity over the Northwest Pacific. *J. Geophys. Res. Atmos.*, **120**, 4072–4089, [CrossRef](#).